LAWRENCE
LIVERMORE
NATIONAL
LABORATORY

UCRL-JRNL-221281

Beyond Spin-Orbit: Probing Electron Correlation in the Pu 5f States

J. G. Tobin

May 10, 2006

Journal of Alloys and Compounds

Beyond Spin-Orbit: Probing Electron Correlation in the Pu 5f States

J.G. Tobin,

Lawrence Livermore National Laboratory,

Livermore, California 94550, USA

ABSTRACT

Experiments planned to address the issue of electron correlation in the Pu 5f states are described herein. The key is the utilization of the Fano Effect, the observation of spin polarization in nonmagnetic systems, using chiral excitation such as circularly polarized X-rays.

Beyond Spin-Orbit: Probing Electron Correlation in the Pu 5f States

I. INTRODUCTION

The enigma of Pu electronic structure is being unraveled. Sixty years after its discovery, the mystery of the electronic structure of Pu is finally being resolved. In a series of experiments and linked theoretical modeling, the range of possible solutions for Pu electronic structure has been dramatically reduced.

The approach is to experimentally determine which potential terms are the largest.

$H\Psi = -(\hbar^2/2m)\nabla^2\Psi + V\Psi$, where $V= V_1 + V_2 + V_3 + V_4 + \ldots$

Synchrotron-radiation-based X-ray absorption, electron energy-loss spectroscopy in a transmission electron microscope, multi-electronic atomic spectral simulations and first principles calculations (Generalized Gradient Approximation in the Local Density Approximation, GGA/LDA) have been used to investigate the electronic structure of Plutonium (Pu). [1-4] From these studies, the following key insights have been gleaned.

1. Russell-Saunders Coupling fails for Pu. Pu is a jj-skewed Intermediate Coupling case, with a large 5f spin-orbit coupling.
2. The number of 5f electrons in Pu is approximately 5.
3. Spin orbit splitting dominates delocalization effects: $V_{SO} > V_{Delocalization}$, to the point that the Pu 5f states can be viewed as predominantly localized.

Beyond Spin-Orbit: Probing Electron Correlation in the Pu 5f States

The remaining issues for Pu electronic structure are primarily those of electron correlation effects. Based upon the success of magnetic methods in explaining the physical properties of the different phases of Pu [5-10], it is possible to hypothesize that for δ-Pu there are strong indications that V_{MAG} perturbs V_{SO} and $V_{MAG} > V_{Delocalization}$. In Pu, it is expected to observe large but counter aligned spin and orbital polarizations or magnetic moments within the 5f manifold. The counter alignment should lead to substantial cancellation. However, there would need to be an additional shielding or cancellation going on in δ-Pu, such as Kondo Shielding [11-13], Spin Fluctuation [14], Non-Collinearity [15], or Averaging [10]. In any case, the magnetic cancellation must be complete: Pu has no net magnetic moment. [16,17] Alternatively, there is the possibility that there are no magnetic substructures and that the electron correlation is a type of pure Kondo shielding best described by Dynamical Mean Field Theory. [11-13] These last two issues can be resolved with the Fano Effect measurements, as will be described below.

The approach is founded upon a model in which magnetic and spin-orbit splittings are included in the picture of the 5f states and upon the observation of chiral/spin-dependent effects in non-magnetic systems. By extending a quantitative model developed for the interpretation of core level spectroscopy in magnetic systems, it is possible to predict the contributions of the individual component states within the 5f manifold. This has lead to a

remarkable agreement between the results of the model and the previously collected spectra of δ-Pu(Ga).

II Estimating the Magnitude of the Magnetic Substructure with XAS

It is important to digress for a moment and reconsider the Pu Density of States (DOS). In a recent PRB [4], Kutepov calculated both a non-magnetic (NM) and Anti-Ferromagnetic (AF) DOS. (Figure 1) Both agree qualitatively with the simple picture derived from spectroscopic results. The NM and AF limits are related, being on opposite ends of the plot below in Figure 1. (For NM, Hs/ζ = 0, and for AF, the extreme limit would be Hs/ζ > 10. Here Hs = Spin Field (Exchange) and ζ = Spin-Orbit Parameter.) The spectrum labeled AF is, in fact, an intermediate solution, where the spin-orbit splitting and exchange splitting are of the same order of magnitude. Is it possible to derive the characteristics of the intermediate solution directly from experimental data?

One way to extract the possible size of the magnetic perturbation would be to analyze the X-ray Absorption Branching Ratio of Pu for the 4d to 5f excitation, assuming a jj limit with a magnetic splitting. This has been done and the result is shown below in Tables 1 and 2 and Figures 2-5. (It should be noted that the EELS results for δ-Pu and α-Pu are essentially identical with each other and with the XAS result for δ-Pu. [3])

There are several steps to this process. First, the orthogonalized initial states must be generated, following the procedure developed previously for shallow core levels in a magnetic system. [18] The resultant states and their energy dependence are shown in Tables 1 and 2 and Figure 2. Next, the state-

to-state matrix elements must be calculated for the case of linearly polarize X-rays, consistent with the experiments performed at the Advanced Light Source. [1-4] To do that, it is necessary to calculate the circular-polarization-driven transition moments (Figure 3) and then sum properly. From there, it is then possible to predict how the Branching Ratio, $B = A_{5/2}/(A_{5/2} + A_{5/2})$ with A as the intensity at each edge, will change as the magnetic effect is increased, as shown in Figure 4.

Thus, the Pu 4d to 5f XAS data (inset in Figure 4) has been analyzed with a simple one electron picture with 5 electrons in the 5f level (n = 5), magnetically polarized 5f states, and linear photon polarization, including the correct state to state transition cross sections within the electric dipole approximation. The branching ratio analysis gives the result that Hs/□ = 2.5. (See Figure 4.) From Kutepov's calculations it is known that $\Delta E_{SO} \approx 2$ eV and using Hs/□ = 2.5, $\Delta E_{MAG} \approx 0.2$ eV is obtained. (See Figure 5)

III Comparison to PES Experimental Results

The new model can explain the "regular" photoemission results for □-Pu. (Figure 6) Using the value of Hs/□ = 2.5 and including the correct state to state transition cross sections within the electric dipole approximation for Photoelectron Spectroscopy (PES), the magnetic perturbation model ($V_{SO} + V_{MAG}$) gives fairly good agreement with our data, bulk □ and bulk □ with a □ reconstruction: at worst, the model result is semi-quantitatively correct. Interestingly, the model is closer to the results of Butterfield et al [19], where the

small remaining oxygen-driven contributions have been reduced even further. Please note that the model has no delocalization nor hybridization in it. In the 5f states, delocalization and hybridization are essentially the same. Thus the result of this analysis suggests that hybridization and delocalization play a role in the δ-Pu 5f states but it is a TERTIARY role…..$V_{SO} > V_{MAG} > V_{Delocalization}$.

Before progressing further, it is useful to consider how the simulated photoelectron spectrum was obtained. Again, state-to-state calculations are performed for the case consistent with the experimental set up, i.e. linear polarization, following the procedure developed earlier [18]. Also again, it begins with the strong selection rules of the circular polarization cases and then summing appropriately. The initial states are the occupied 5f states with the energy dependences shown in Figure 2. The possible intensity for each state will depend upon the value of Hs/δ, as shown in Figure 7. For δ-Pu, it is assumed that the occupancy is 5.1. [5] Thus, States 14, 13, 12, 11, and 10 are fully occupied and State 9 is only partially occupied (0.1) and tied to the Fermi Energy. Only occupied states will contribute to PES, each in proportion to its occupation. The final state is a plane wave at normal emission, directed into the electron analyzer. Both final states, d –wave and g-wave, were considered, as shown in Table 2. (It is also possible to obtain spin dependent dichroisms for each state, as well as a preliminary estimate of the magnetic moments, as shown in Figure 7. The spin dichroisms will be discussed in more detail below.) To obtain a spectrum, however, it is also necessary to have an estimate of (1)

peak shape and (2) the energy placement of the states. Here, a Doniach-Sunjic lineshape (Figure 8) has been used, for each specific occupied initial state. The parameters used followed the guidelines below.

1. The DS-asymmetry parameter was 0.3 throughout.
2. The Intensity and Dichroism values for each state, 9 through 14, were kept constant throughout. The values used corresponded to the case of Hs/Γ << 1 and for the f to d transition. By using the values corresponding to Hs/Γ << 1, the effect of errors in the determination of Hs/Γ are minimized. As shown in Table 3, the matrix elements for the f to g-wave and f to d-wave are very similar for the Intensities and differ only by a negative sign in the Dichroism.
3. The lifetime peak-width value was extracted from the experimental Am He-II spectrum of Naegele. [20] The lifetime values were proportional to the Am value and allowed to diminish linearly to zero as binding energy went to zero, for each individual state.
4. The tentative “exchange splitting” value was extracted from our experimental Pu XAS spectrum, as described above, with an effective value of approximately 0.2 eV.
5. No further optimization of parameters was performed.

IV Spin Polarized PES Measurements

The acid test of the new model of Pu electronic structure will be the spin dependence. Using the Fano Effect (Double Polarization Photoelectron

Dichroism), a strong spin dependence in Non-Magnetic Pu should be observed, as shown in Figure 9. The Fano Effect is the emission of spin polarized electrons by NONMAGNETIC materials, when excited by circularly polarized photons, as predicted by U. Fano [21] and measured shortly thereafter. [22-24] Fano Dichroism PES is the ideal technique with which to probe for such a dynamically shielded moment, with (1) a probe time on the scale of 10^{-18} seconds and (2) the capability to see spin effects in nonmagnetic materials.

At this point, it is useful to digress again and consider the "Fano Effect" and its special characteristics in more detail. It is believed that Fano effect measurements (aka Double Polarization Photoelectron Spectroscopy, DPPS) are the key to unraveling the electron correlation in Pu. In Fano Effect measurements, one uses a chiral excitation and true spin detection of the electrons in NONMAGNETIC materials to gain detailed information about the valence band electronic structure of these materials. In ferro-magnetic systems, it is only necessary to have only single polarization because of the presence of the macroscopic magnetization vector. In the case of ferro-magnetic systems with a double polarization experiment, the major improvement is in increasing the magnitude of the observed effects, at the cost of raw signal rate. In non-magnetic systems with single polarization, no effect is observed. In order to see the underlying spin characteristics in non-magnetic systems, one must resort to double polarization experiments. (Figure 10)

The Pu spectrum shown in Figure Figure 9 is a simulated spin dichroism spectrum, based upon the theoretical model developed in Section III and

illustrated in Figures 6-8. As a test of this model, it has also been applied to he case of the Au 4f Fano Effect, as shown in Figure 11. Clearly, even with this simple model the essence of the spin dichroic behavior is captured, generating almost quantitative agreement with the experimental results.

The investigation is being pursued in a two-pronged fashion: (a) calibration studies of Ce, the 4f analogue of Pu, at synchrotron radiation sources; and (b) in house studies of Pu.

Although we have not yet been able to carry out the Pu Double Polarization experiment, we have been able to test the feasibility of this approach using Ce, the Rare Earth element analog of Pu. Shown in Figure 12 are the preliminary results for Double Polarization Photoelectron Spectroscopy of polycrystalline □□Ce, using both a chiral excitation source (such as circularly polarized x-rays) and spin resolving detection. [25-27]

V Pu Summary:

The correct Hamiltonian for Pu is being converged upon.

Proven: Pu is a jj-skewed Intermediate Coupling case, NOT LS (Russell-Saunders).

Proven: $V_{SO} >> V_{Delocalization}$

Strong Indications for □-Pu: V_{MAG} perturbs V_{SO} and $V_{MAG} > V_{Delocalization}$

Possibly: There is an additional cancellation going on in □-Pu, such as Kondo Shielding, Spin Fluctuation, Non-Collinearity, or Averaging.

We can resolve these last two issues with the Fano Effect measurements.

Probable ordering

□-Pu 5f : $V_{SO} > V_{MAG} \approx V_{Delocalization} > 0$.

□-Pu 5f : $V_{SO} > V_{MAG} > V_{Delocalization} > 0$.

Beyond Spin-Orbit: Probing Electron Correlation in the Pu 5f States

Acknowledgements
This work was performed under the auspices of the U.S. DOE by University of California Lawrence Livermore National Laboratory under contract W-7405-Eng-48.

References

1. J.G. Tobin, B.W. Chung, R. K. Schulze, J. Terry, J. D. Farr, D. K. Shuh, K. Heinzelman, E. Rotenberg, G.D. Waddill, and G. Van der Laan, Phys. Rev. B **68**, 155109 (2003).
2. K.T. Moore, M.A. Wall, A.J. Schwartz, B.W. Chung, D.K. Shuh, R.K. Schulze, and J.G. Tobin, Phys. Rev. Lett. **90**, 196404 (2003).
3. G. van der Laan, K.T. Moore, J.G. Tobin, B.W. Chung, M.A. Wall, and A.J. Schwartz, Phys. Rev. Lett. **93**, 097401 (2004); K. T. Moore, G. van der Laan, R. G. Haire, M. A. Wall, and A. J. Schwartz, Phys. Rev. B **73**, 033109 (2006).
4. J.G. Tobin, K.T. Moore, B.W. Chung, M.A. Wall, A.J. Schwartz, G. van der Laan, and A.L. Kutepov, Phys. Rev. B **72**, 085109 (2005).
5. S.Y. Savrosov and G. Kotliar, Phys. Rev. Lett. **84**, 3670 (2000).
6. P. Soderlind, EuroPhysics Letters **55**, 525 (2001).
7. P. Soderlind, A. Landa, and B. Sadigh, Phys. Rev. B **66**, 205109 (2002).
8. B. Sadigh, P. Soderlind,and W.G. Wolfer, Phys. Rev. B **68**, 241101 (2003).
9. P. Soderlind and B. Sadigh Phys. Rev. Lett. **92**, 185702 (2004).

10. A.L. Kutepov and S.G. Kutepova J.Phys. Cond. Matter **15**, 2607 (2003); A.L. Kutepov, private communication, UCRL-TR-200654.
11. G. Kotliar and D. Vollhardt, Physics Today **57,** 53 (March 2004).
12. R.C. Albers, *Nature* **410**, 759 (2001).
13. S.Y. Savrasov, G. Kotliar, E. Abrahams, *Nature* **410**, 793 (2001).
14. A.J. Arko, M.B. Brodsky and N.J. Nellis, Phys. Rev. B **5**, 4564 (1972).
15. Michael Brookes, ITU, Germany, private communication.
16. J. Lashley, A. Lawson, R.B. McQueeney, and G.H. Lander, Phys. Rev. B **72**, 054416 (2005) and references therein.
17. W.J. Nellis, and M.B. Brodsky, "Magnetic Properties," in The Actinides: Electronic Structure and Related Properties, Vol.2, ed. A.J. Freeman and S. Darby, (Academic, New York, 1974).
18. J.G. Tobin and F.O. Schumann, Surface Science **478**, 211 (2001).
19. M.T.Butterfield, T.Durakiewicz, E. Guziewicz, J.J.Joyce, A.J.Arko, D.P.Moore and L.Morales, Surface Science **571**, 74 (2004).
20. J. R. Naegele, L. Manes, J. C. Spirlet, and W. Müller, Phys. Rev. Lett. **52**, 1834-1837 (1984).
21. U. Fano, Phys. Rev. **178**, 131 (1969); **184**, 250 (1969).
22. J. Kessler and J. Lorenz, Phys. Rev. Lett. 24, 87 (1970).
23. G. Baum, M.S. Lubell, and W. Raith, Phys. Rev. Lett. 25, 267 (1970).
24. U. Heinzmann, J. Kessler, and J. Lorenz, Phys. Rev. Lett. 25, 1325 (1970).

25. S.W. Yu, T. Komesu, B.W. Chung, G.D. Waddill, S.A. Morton, and J.G. Tobin, Phys. Rev. B **73**, 075116 (2006).

26. J.G. Tobin, S.A. Morton, B.W. Chung, S.W. Yu and G.D. Waddill, Physica B **378-380**, xxxxx (May 2006).

27. J.G. Tobin, S.W. Yu, T. Komesu, B.W. Chung, S.A. Morton and G.D. Waddill, "Proof of Dynamical Spin Shielding in Ce from Spin-Resolved Photoelectron Spectroscopy," UCRL-JRNL-220635.

Beyond Spin-Orbit: Probing Electron Correlation in the Pu 5f States

Table 1 Orthogonalized Initial 5f states

$|1\rangle = |3, 1/2\rangle$

$|2\rangle = \cos\theta_2 |2, 1/2\rangle + \sin\theta_2 |3, -1/2\rangle$

$|3\rangle = \cos\theta_3 |1, 1/2\rangle + \sin\theta_3 |2, -1/2\rangle$

$|4\rangle = \cos\theta_4 |0, 1/2\rangle + \sin\theta_4 |1, -1/2\rangle$

$|5\rangle = \cos\theta_5 |-1, 1/2\rangle + \sin\theta_5 |0, -1/2\rangle$

$|6\rangle = \cos\theta_6 |-2, 1/2\rangle + \sin\theta_6 |-1, 1/2\rangle$

$|7\rangle = \cos\theta_7 |-3, 1/2\rangle + \sin\theta_7 |-2, -1/2\rangle$

$|8\rangle = |-3, -1/2\rangle$

$|9\rangle = -\sin\theta_7 |-3, 1/2\rangle + \cos\theta_7 |-2, -1/2\rangle$

$|10\rangle = -\sin\theta_6 |-2, 1/2\rangle + \cos\theta_6 |-1, -1/2\rangle$

$|11\rangle = -\sin\theta_5 |-1, 1/2\rangle + \cos\theta_5 |0, -1/2\rangle$

$|12\rangle = -\sin\theta_4 |0, 1/2\rangle + \cos\theta_4 |1, -1/2\rangle$

$|13\rangle = -\sin\theta_3 |1, 1/2\rangle + \cos\theta_3 |2, -1/2\rangle$

$|14\rangle = -\sin\theta_2 |2, 1/2\rangle + \cos\theta_2 |3, -1/2\rangle$

$2\theta_2 = \arctan (2.4995/ (2.5 + H_S/\zeta)) \geq 0$

$2\theta_3 = \arctan (3.1623/ (1.5 + H_S/\zeta)) \geq 0$

$2\theta_4 = \arctan (3.4641/ (0.5 + H_S/\zeta)) \geq 0$

$2\theta_5 = \arctan (3.4641/ (-0.5 + H_S/\zeta)) \geq 0$

$2\theta_6 = \arctan (3.1623/ (-1.5 + H_S/\zeta)) \geq 0$

$2\theta_7 = \arctan (2.4995/ (-2.5 + H_S/\zeta)) \geq 0$

Beyond Spin-Orbit: Probing Electron Correlation in the Pu 5f States

Table 2 Energies of the orthogonalized 5f states

$E_1 = H_S/\zeta * 0.5 + 1.5$

$E_2 = H_S/\zeta *(-0.5 + (\cos\theta_2)^2) + 1.0*(\cos\theta_2)^2 - 1.5*(\sin\theta_2)^2 + (\cos\theta_2)*(\sin\theta_2)*2.4495$

$E_3 = H_S/\zeta *(-0.5 + (\cos\theta_3)^2) + 0.5*(\cos\theta_3)^2 - 1.0*(\sin\theta_3)^2 + (\cos\theta_3)*(\sin\theta_3)*3.1623$

$E_4 = H_S/\zeta *(-0.5 + (\cos\theta_4)^2) + 0*(\cos\theta_4)^2 - 0.5*(\sin\theta_4)^2 + (\cos\theta_4)*(\sin\theta_4)*3.4641$

$E_5 = H_S/\zeta *(-0.5 + (\cos\theta_5)^2) - 0.5*(\cos\theta_5)^2 - 0*(\sin\theta_5)^2 + (\cos\theta_5)*(\sin\theta_5)*3.4641$

$E_6 = H_S/\zeta *(-0.5 + (\cos\theta_6)^2) - 1.0*(\cos\theta_6)^2 + 0.5*(\sin\theta_6)^2 + (\cos\theta_6)*(\sin\theta_6)*3.1623$

$E_7 = H_S/\zeta *(-0.5 + (\cos\theta_7)^2) - 1.5*(\cos\theta_7)^2 + 1.0*(\sin\theta_7)^2 + (\cos\theta_7)*(\sin\theta_7)*2.4495$

$E_8 = -H_S/\zeta * 0.5 + 1.5$

$E_9 = -H_S/\zeta *(-0.5 + (\cos\theta_7)^2) - 1.5*(\sin\theta_7)^2 + 1.0*(\cos\theta_7)^2 - (\cos\theta_7)*(\sin\theta_7)*2.4495$

$E_{10} = -H_S/\zeta *(-0.5 + (\cos\theta_6)^2) - 1.0*(\sin\theta_6)^2 + 0.5*(\cos\theta_6)^2 - (\cos\theta_6)*(\sin\theta_6)*3.1623$

$E_{11} = -H_S/\zeta *(-0.5 + (\cos\theta_5)^2) - 0.5*(\sin\theta_5)^2 - 0*(\cos\theta_5)^2 - (\cos\theta_5)*(\sin\theta_5)*3.4641$

$E_{12} = -H_S/\zeta *(-0.5 + (\cos\theta_4)^2) + 0*(\sin\theta_4)^2 - 0.5*(\cos\theta_4)^2 - (\cos\theta_4)*(\sin\theta_4)*3.4641$

$E_{13} = -H_S/\zeta *(-0.5 + (\cos\theta_3)^2) + 0.5*(\sin\theta_3)^2 - 1.0*(\cos\theta_3)^2 - (\cos\theta_3)*(\sin\theta_3)*3.1623$

$E_{14} = -H_S/\zeta *(-0.5 + (\cos\theta_2)^2) + 1.0*(\sin\theta_2)^2 - 1.5*(\cos\theta_2)^2 - (\cos\theta_2)*(\sin\theta_2)*2.4495$

$2\theta_2 = \arctan (2.4995/ (2.5 + H_S/\zeta)) \geq 0$

$2\theta_3 = \arctan (3.1623/ (1.5 + H_S/\zeta)) \geq 0$

$2\theta_4 = \arctan (3.4641/ (0.5 + H_S/\zeta)) \geq 0$

$2\theta_5 = \arctan (3.4641/ (-0.5 + H_S/\zeta)) \geq 0$

$2\theta_6 = \arctan (3.1623/ (-1.5 + H_S/\zeta)) \geq 0$

$2\theta_7 = \arctan (2.4995/ (-2.5 + H_S/\zeta)) \geq 0$

Table 3

Here are shown the PES Intensity magnitudes (M_L) for linearly polarized excitation and Spin Dichroisms (D_C) for circularly polarized excitation, for a final state of g wave and f wave character. Relative intensities between columns depends upon various radial matrix elements and is thus photon energy dependent.

Each column normalized such that the largest value equals one.

m_{5f}	M_L^g	D_C^g	M_L^d	D_C^d
3	1	-1	1	1
2	0	0	0	0
1	0.318	-1/5	0.244	1/5
0	0	0	0	0
-1	0.318	1/5	0.244	-1/5
-2	0	0	0	0
-3	1	1	1	-1

Beyond Spin-Orbit: Probing Electron Correlation in the Pu 5f States

Figure 1

Simple Picture derived from the spectroscopic analysis

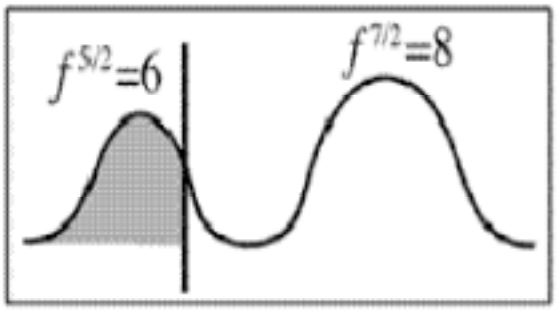

Result of non-magnetic calculation, including spin-orbit in the Pu 5f's

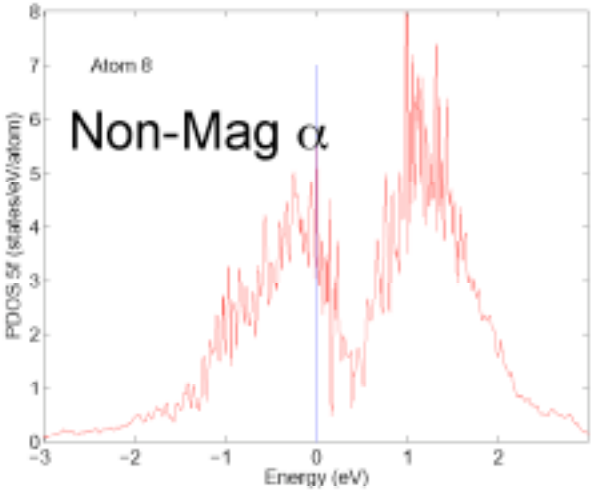

Result of anti-ferromagnetic calculation, including spin-orbit in the Pu 5f's

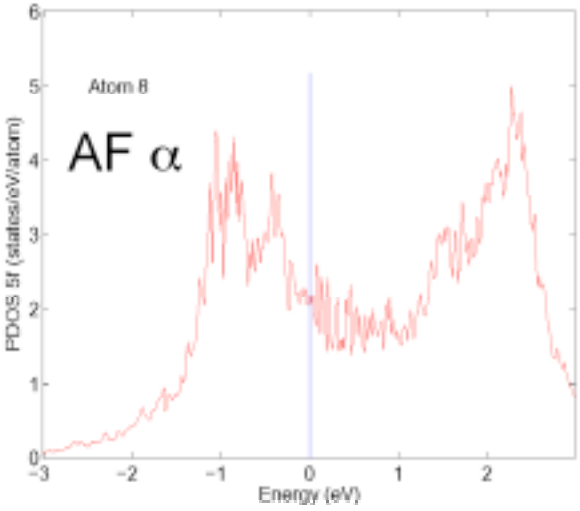

Beyond Spin-Orbit: Probing Electron Correlation in the Pu 5f States

Figure 2
Here is a picture of the energy of the orthogonalized states as a function of the ratio of the exchange and spin orbit splittings. Hs is the "spin field" or exchange splitting between states 1 and 8. (The states are numbered 1-14, starting at the top.) □ is the spin-orbit splitting parameter. For Th through Am, only the lower states, 14 through 9, will be occupied .

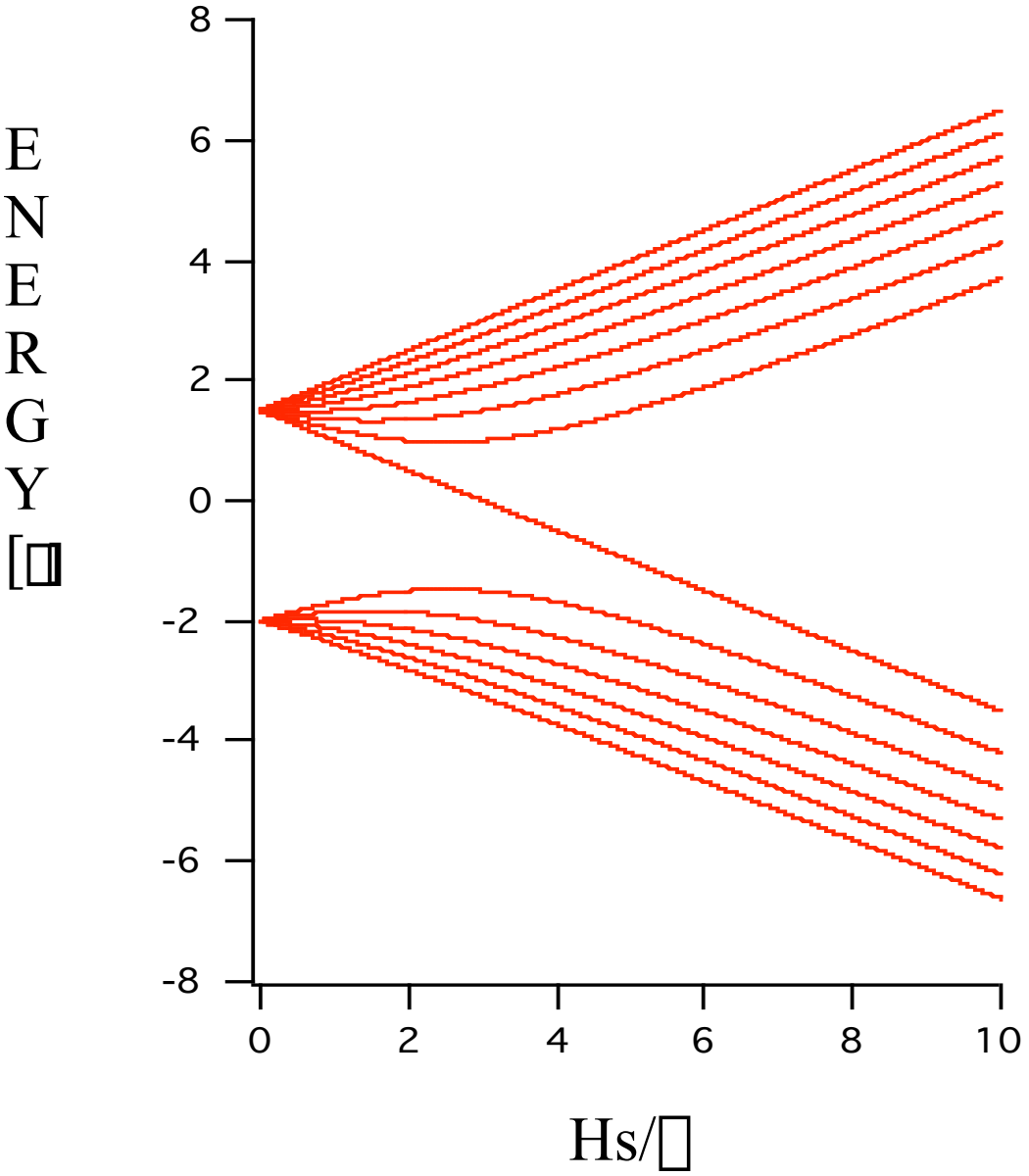

Beyond Spin-Orbit: Probing Electron Correlation in the Pu 5f States

Figure 3a
Schematic illustration of the x-ray absorption process. E_F is the Fermi Level, the energy level between the occupied and unoccupied states. The photon (h□) is absorbed, moving the core level electron (e-) up into the unoccupied states.

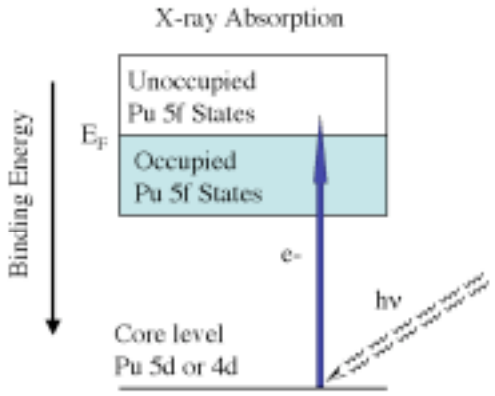

Figure 3b
Example of XAS electric dipole transitions for pure spin orbit split states.

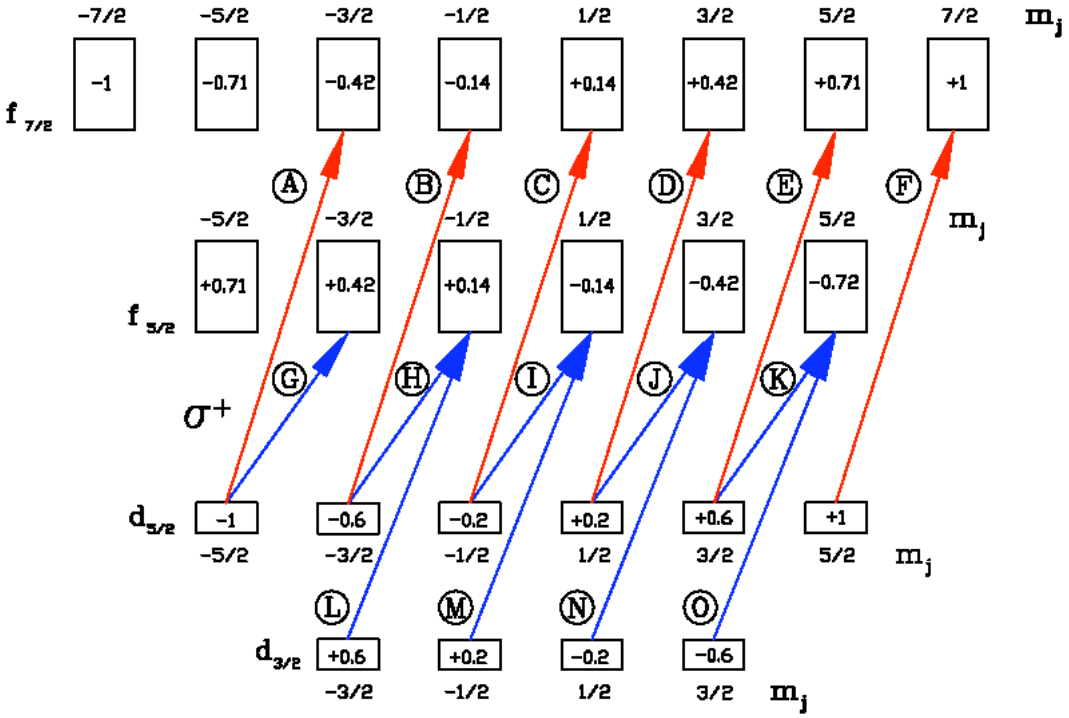

Scheme of the photoexcitation d to f with positive helicity . The arrows indicate the allowed transitions via relativistic dipole selection rules for positive helicity with the following transition probabilities normalized to transition G. A=5/2, B=15/2, C=30/2, D=50/2, E=75/2, F=105/2, G=1, H=8/5, I=9/5, J=8/5, K=1, L=49/10, M=147/10, N=147/5, O=49. Thereby, identical radial parts of the $d_{5/2}$ and $d_{3/2}$ wave functions and of the $f_{7/2}$ and $f_{5/2}$ wave functions are assumed. The arrows with red (blue) color represent transitions which give positive (negative) spin polarization of photoelectrons. Positive and negative numbers in the rectangles give the angle integrated spin polarization for given mj using Clebsch-Gordan coefficients. Energy differences are not to scale. For more detail, see reference 24. Note that $d_{3/2}$ to $f_{7/2}$ transitions are forbidden for pure spin orbit split states. Courtesy of Sung Woo Yu.

Beyond Spin-Orbit: Probing Electron Correlation in the Pu 5f States

Figure 4
Here is shown the experimental determination of the Hs/ratio from the experimental XAS Pu branching ratio (B) and a simple model including the effect of both spin-orbit splitting and magnetic splitting.

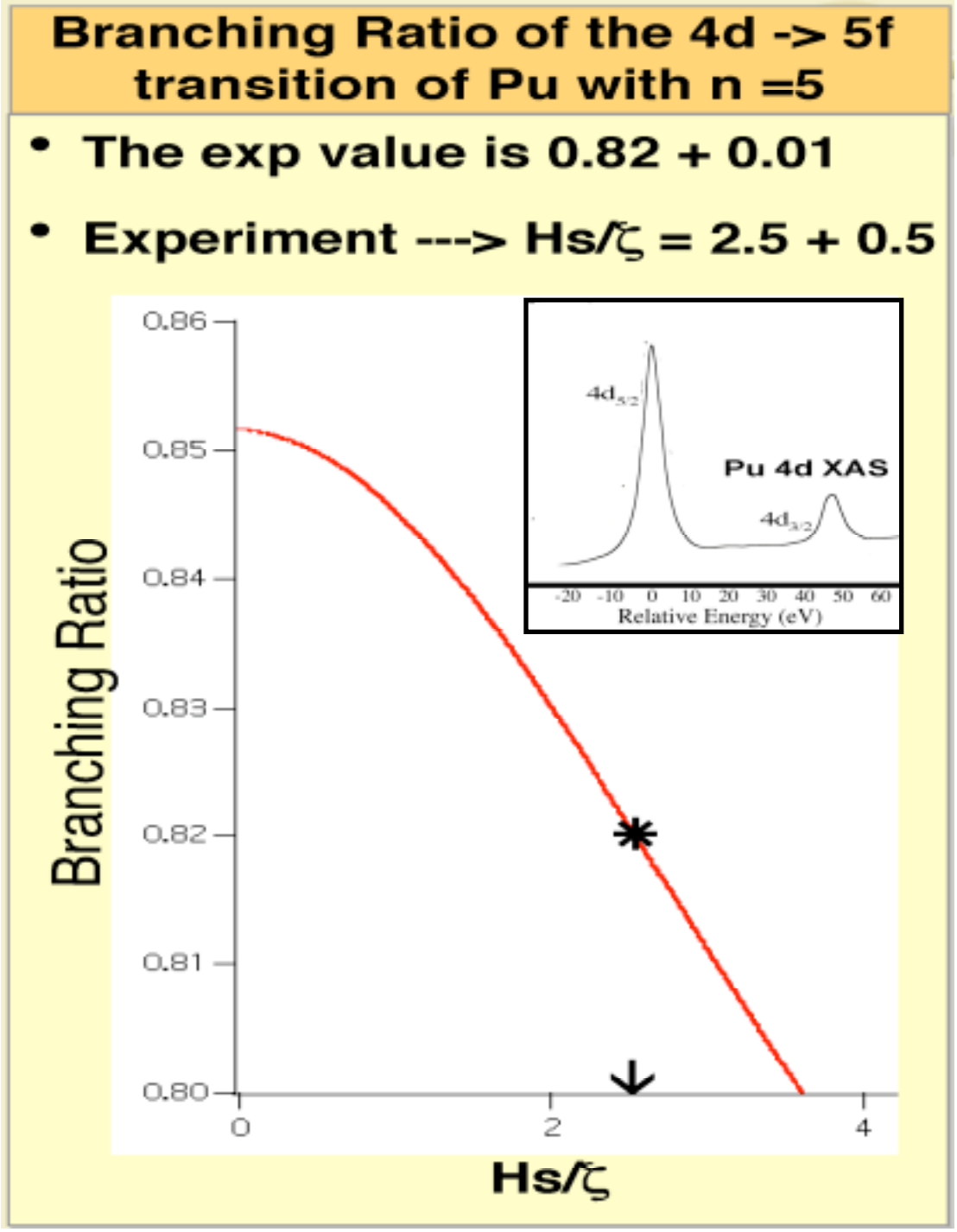

Beyond Spin-Orbit: Probing Electron Correlation in the Pu 5f States

Figure 5
Shown here are the energy values of the orthogonalized 5f component states (in units of □) as a function of the ratio of exchange (Hs) and spin orbit (□) splittings. At Hs/□ = 2.5, □E_{MAG} ≈ 0.2 eV, from □ ≈ 0.57 eV, □E_{SO} ≈ 2 eV and □E_{SO} = 7□/2.

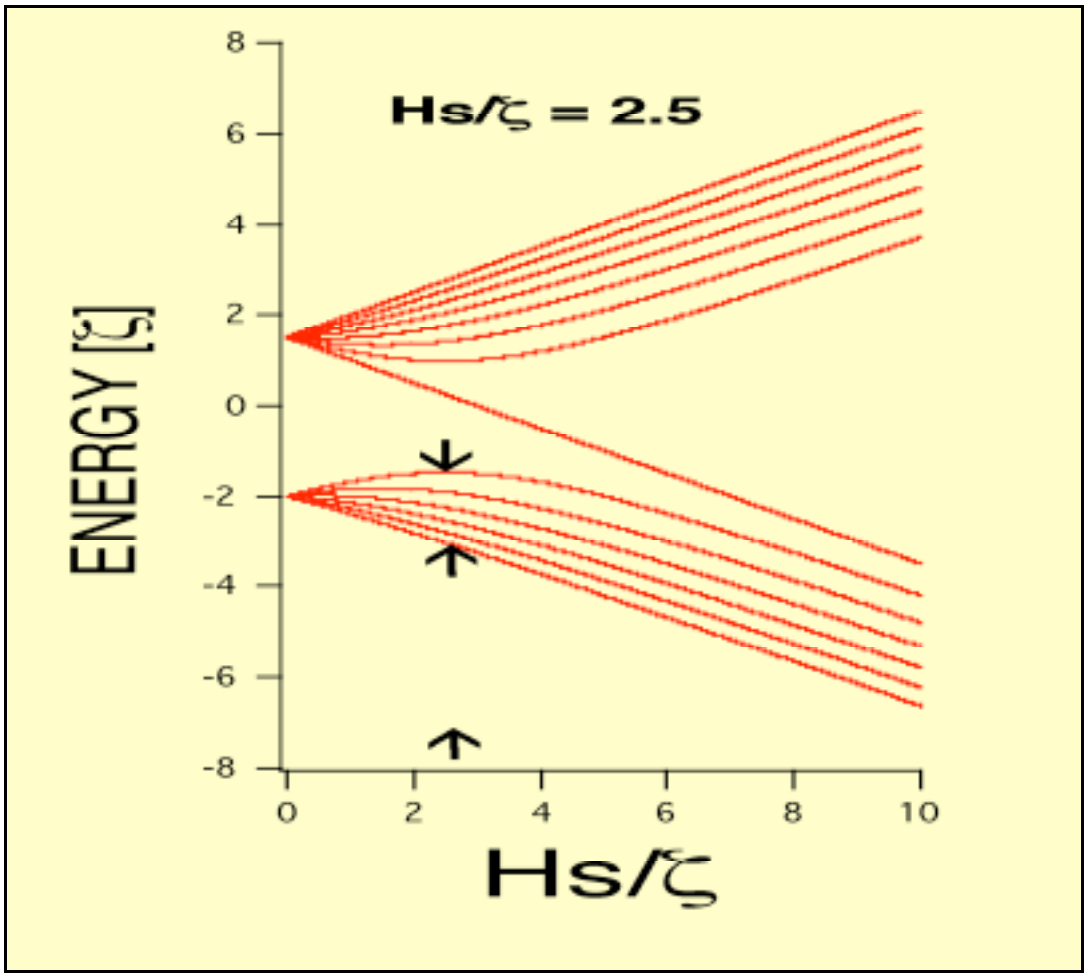

Beyond Spin-Orbit: Probing Electron Correlation in the Pu 5f States

Figure 6
Photoelectron Spectroscopy (PES) Experiment and Theory are shown here. The theory here is NOT Density of States (DOS) but rather spectral simulations with correct state-to-state matrix elements.

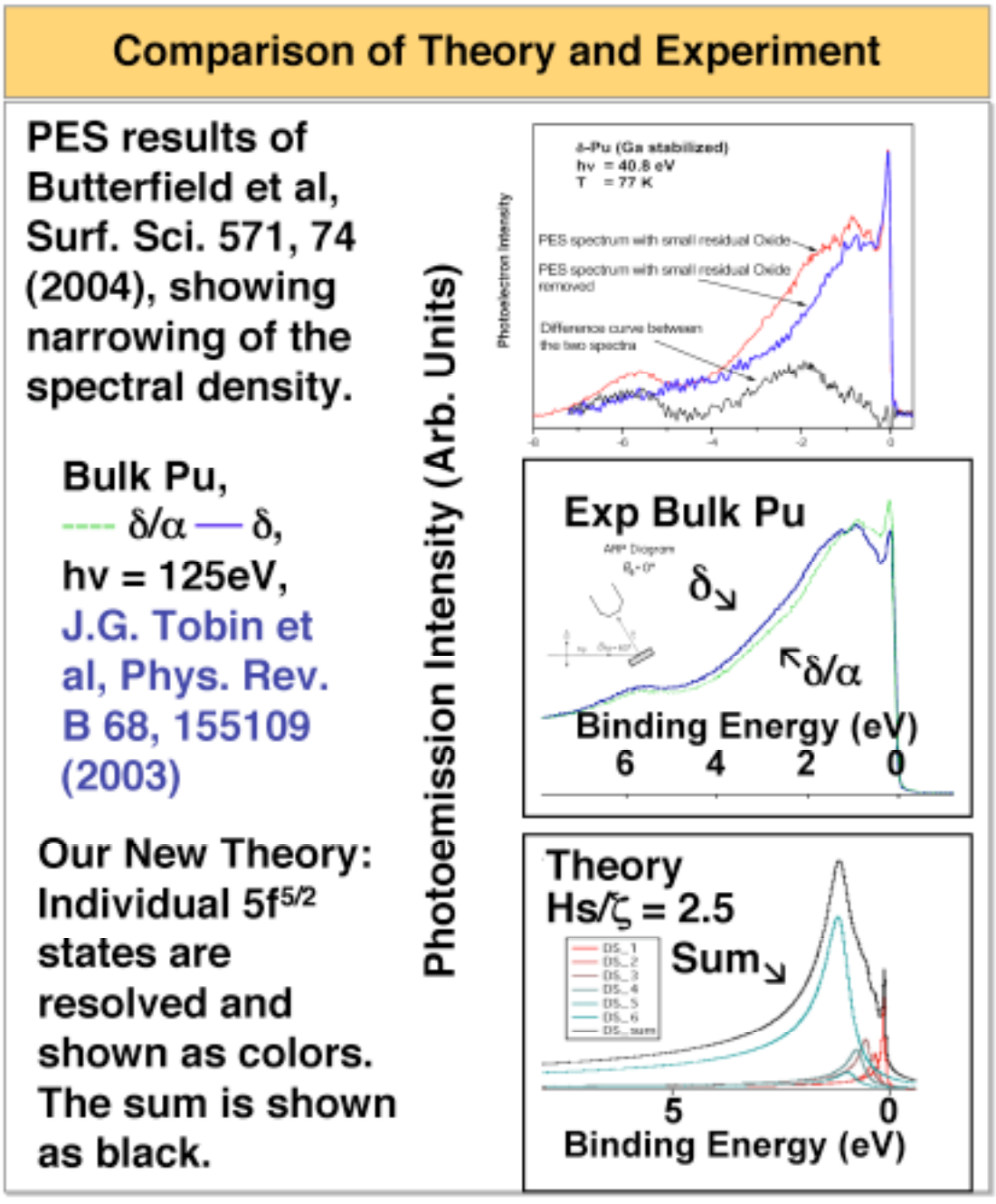

Beyond Spin-Orbit: Probing Electron Correlation in the Pu 5f States

Figure 7
Shown here are predictions of strong intensities and reversed dichroisms from states 9 and 14, for f to d-wave transitions. Similar results occur for the f to g transitions (not shown). Hs/□ is the Exchange/Spin Orbit Splitting ratio. From the model, one can calculate the 5f spin, 5f orbital and 5f total moments versus Hs/□, assuming the Pu 5f electrons are metallic and do not experience angular momentum coupling,i.e., following Savrosov and Kotliar. [5]

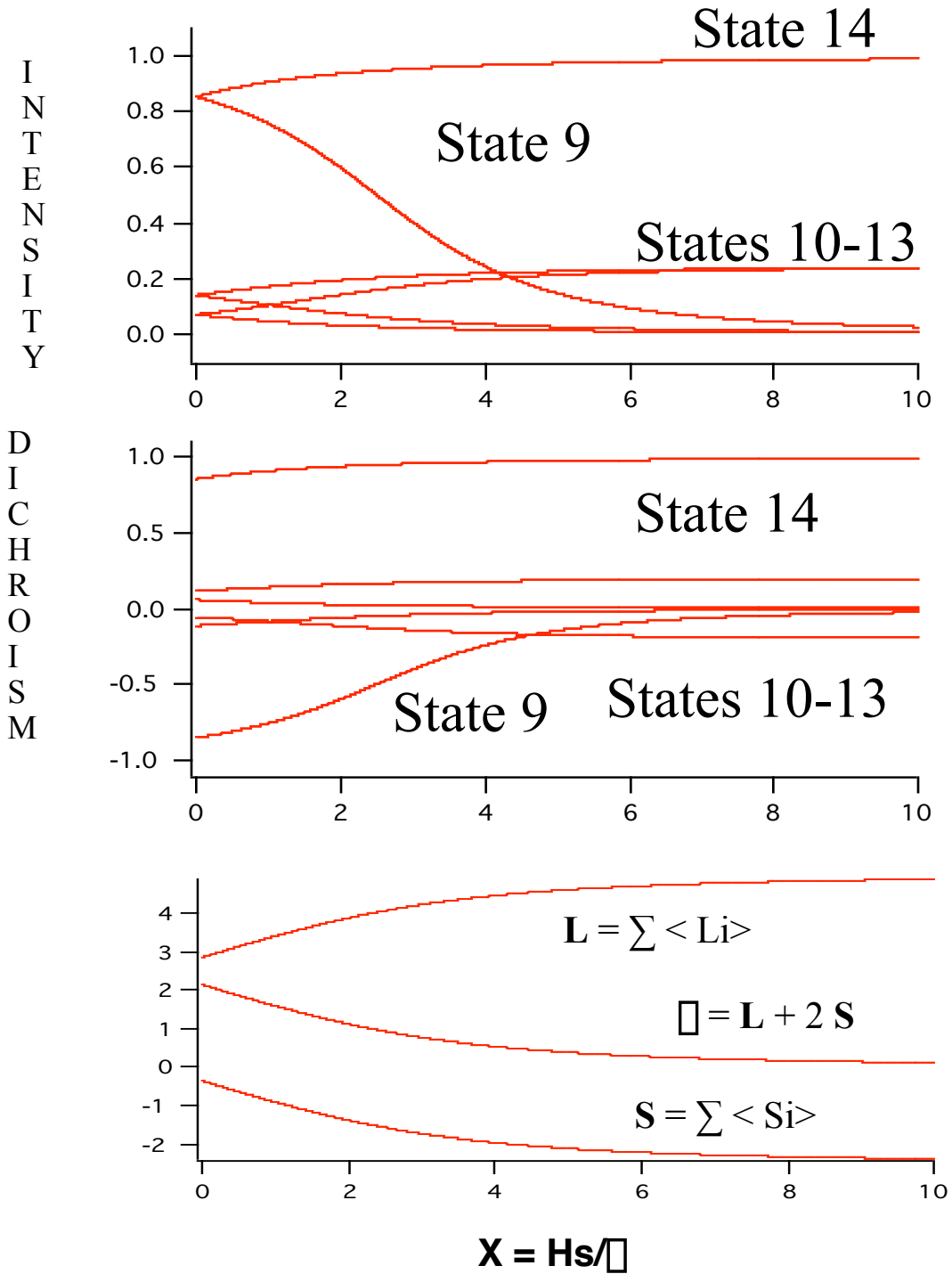

Figure 8
Shown here are the (a) DS line-shapes and (b) the DS asymmetry.

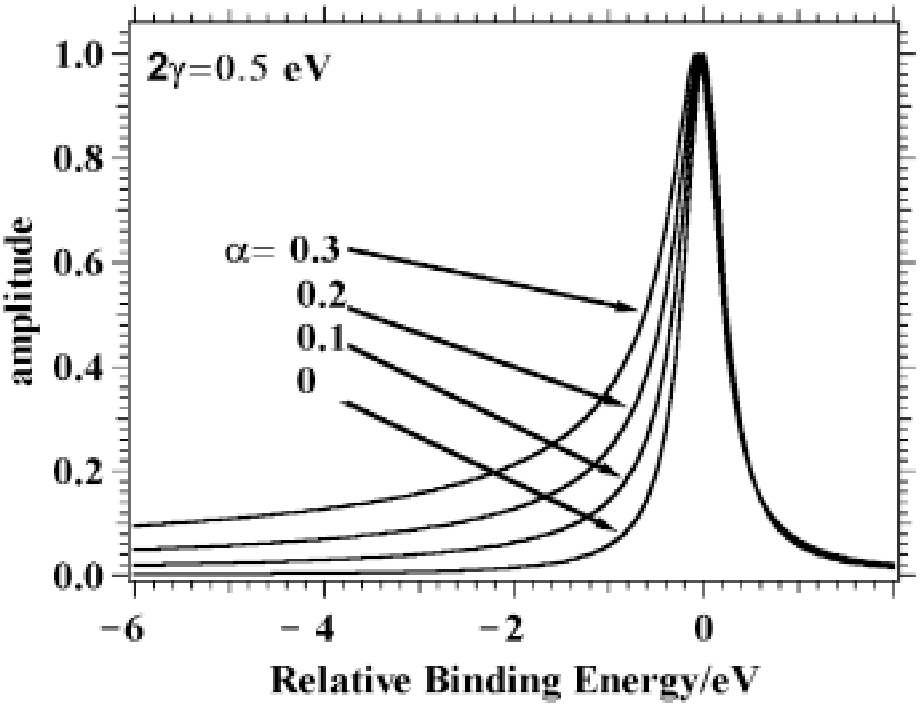

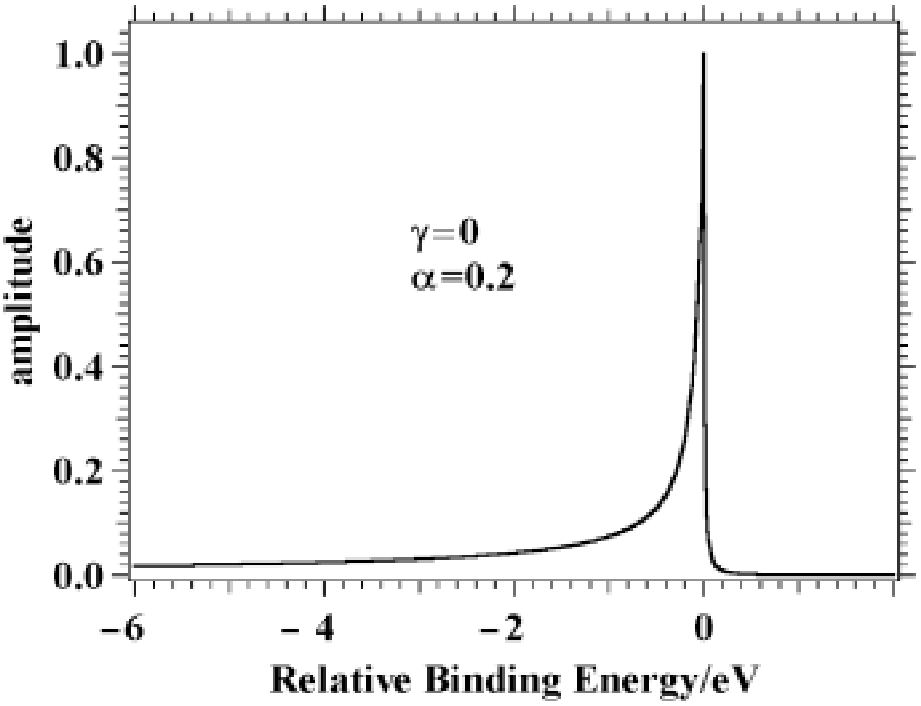

Beyond Spin-Orbit: Probing Electron Correlation in the Pu 5f States

Figure 9
Above is our prediction of the dichroism in □-Pu. Double Polarization Photoelectron Dichroism is the ideal technique with which to probe for such a dynamically shielded moment, with (1) a probe time on the scale of 10^{-18} seconds and (2) the capability to see spin effects in nonmagnetic materials.

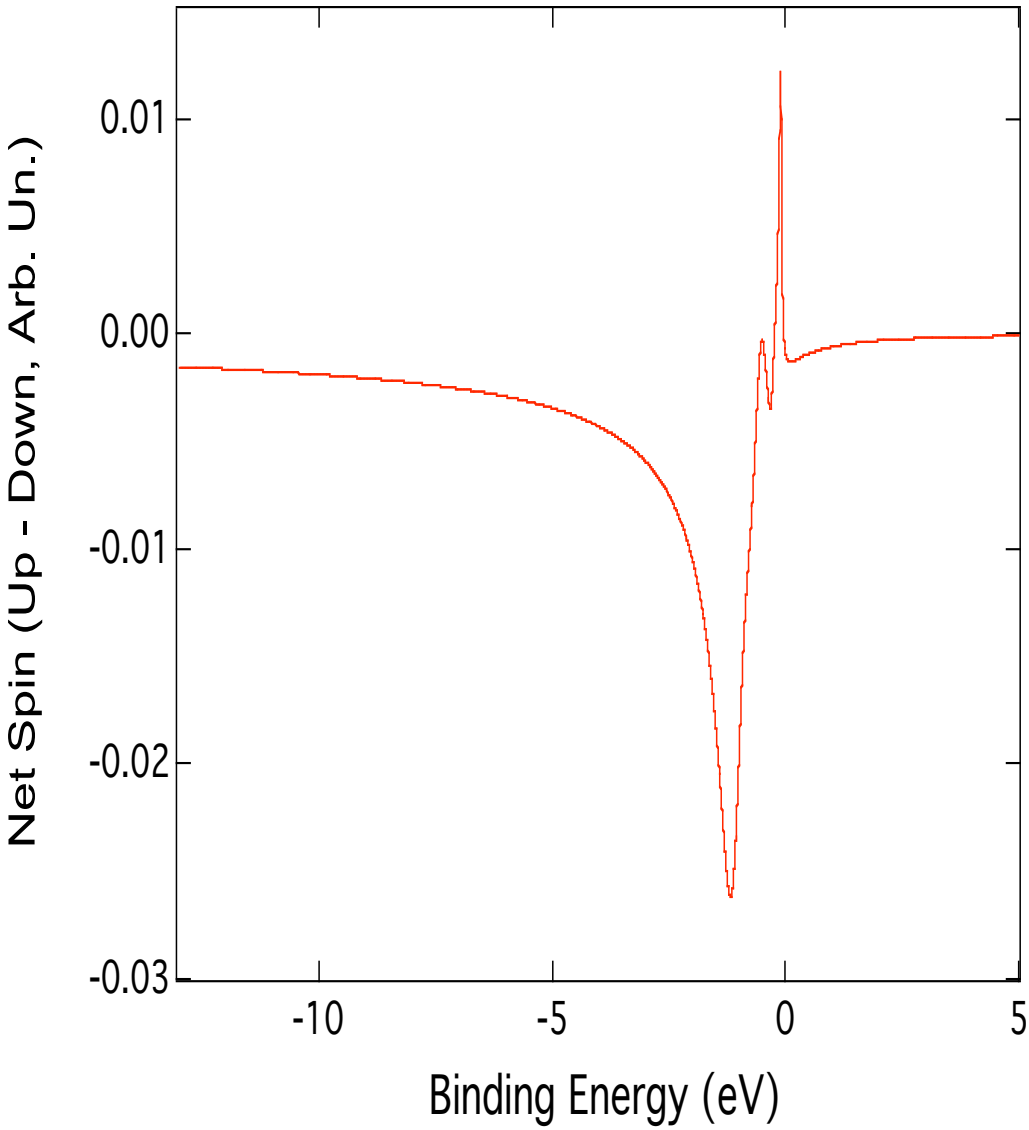

Beyond Spin-Orbit: Probing Electron Correlation in the Pu 5f States

Figure 10
Top, left- unpolarized;
Bottom, left- single polarization due to circularly polarized x-rays;
Top, right- single polarization due to spin detection;
Bottom, right- double polarization photoelectron dichroism.
It should be noted that although the "unpolarized" case with linear polarization is shown, it is possible to use linearly polarized or unpolarized x-radiation as part of a chiral arrangement, to achieve X-ray Magnetic Linear Dichroism in PES. Here the chiral arrangement of vectors essentially mimics the intrinsic chirality of the circularly polarized x-rays

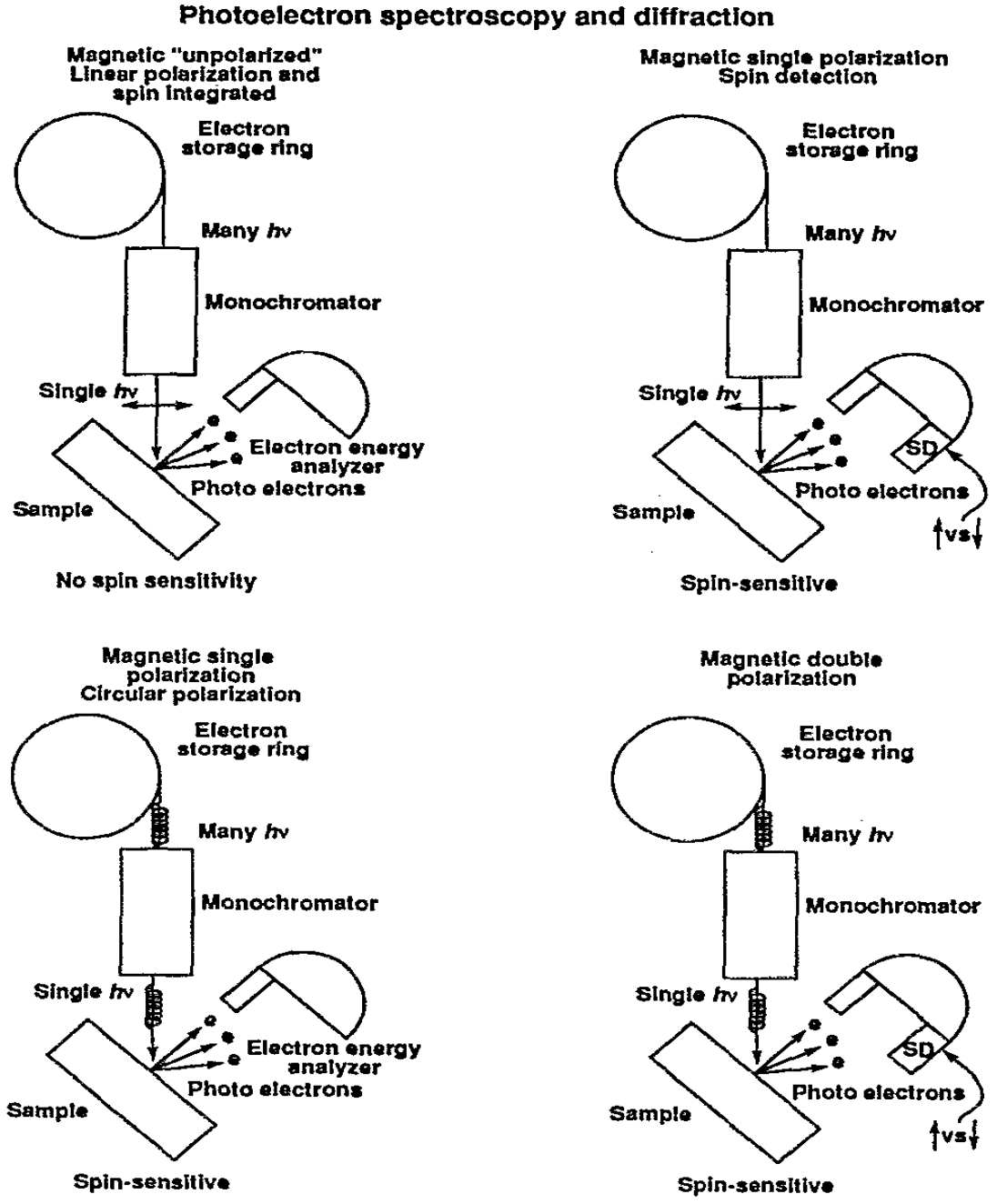

Beyond Spin-Orbit: Probing Electron Correlation in the Pu 5f States

Figure 11
Shown here are the experimental results for the Au 4f states, without background subtraction, as well as the results of the model.

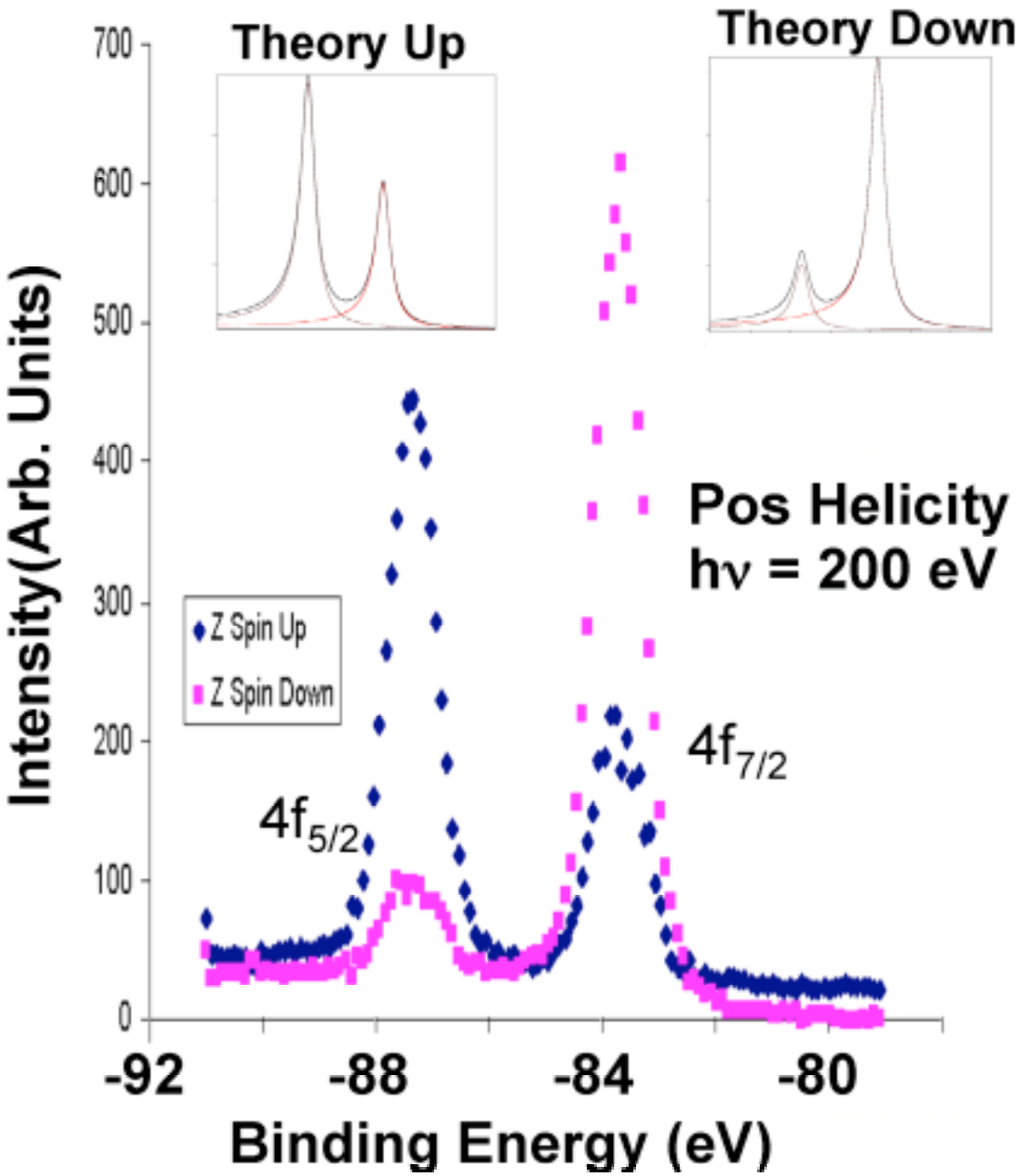

Figure 12 Fano PES results from Ce, from Ref 26.